ANNALS OF PHYSICS: 5, 156–181 (1958)

Long-lived Neutral K Mesons*

M. BARDON, K. LANDE, AND L. M. LEDERMAN

Columbia University, New York, New York, and Brookhaven National Laboratories, Upton, New York

AND

WILLIAM CHINOWSKY

Brookhaven National Laboratories, Upton, New York

The results of a complete analysis of photographs obtained by the Columbia 36-in. magnet cloud chamber in neutral beams of the Brookhaven Cosmotron are presented. A "short-distance" exposure yielded 152 events giving unambiguous proof of the existence of long-lived neutral V-particles, most naturally interpreted as examples of K_2^0 disintegrations. In a subsequent "long-distance" run, 34 events were found, giving a lifetime for K_2^0 of $8.1_{-2.4}^{+3.2} \times 10^{-8}$ sec. Decay modes identified were: $\pi^{\pm}e^{\mp}$ plus a neutral; $\pi^{\pm}\mu^{\mp}$ plus a neutral and $\pi^+\pi^-$ plus a neutral. These are most economically interpreted as the neutral counterparts of K^+ decay, i.e., $\pi^{\pm}e^{\mp}\nu$, $\pi^{\pm}\mu^{\mp}\nu$, and $\pi^+\pi^-\pi^0$. In this case, the first two constitute the bulk of the events, the τ^0 mode being $\lesssim 15\%$ of the total sample. No evidence is found for 2-body disintegrations. Finally, the recent literature on the subject of K_2^0 is briefly reviewed.

I. HISTORICAL INTRODUCTION

Among the known elementary particles, the K^0 is unique. It and its antiparticle, though not identical, are indistinguishable by observation of their decay. The consequences of this novel situation were first explored by Pais and Gell-Mann (*1*). Essential to their argument was the assumption of rigorous charge conjugation invariance in the decay process. Since the K^0 and its charge conjugate $\bar{K}^0$ are not eigenstates of the charge conjugation operator, linear combinations

$$\psi_1 = \frac{K^0 + \bar{K}^0}{\sqrt{2}},$$

$$\psi_2 = \frac{K^0 - \bar{K}^0}{\sqrt{2}\,i}$$

* This research is supported by the Office of Naval Research and the Atomic Energy Commission.

were introduced, for which charge conjugation quantum numbers are defined. It was suggested that the ψ_1 , ψ_2 fields rather than the K^0, $\bar{K}^0$ correspond to observed neutral K particles with definite lifetime. The fields ψ_1 and ψ_2 do not have a defined strangeness. Production of K^0 or $\bar{K}^0$ would then be described as creation with equal probability and prescribed relative phase of either K_1^0 or K_2^0, the quanta of the ψ_1 , ψ_2 fields. The permitted decay modes for K_1^0 and K_2^0 are quite different. Since the two-pion state has definite charge conjugation quantum number, only one of the mixed states ψ_1 or ψ_2 can undergo the observed decay into π^+ and π^-. The other particle must decay into other states, for instance $\pi^+ + \pi^- + \gamma$, of opposite behavior under charge conjugation. For this particle the decay into two pions is forbidden. Simple considerations lead to the conclusion that the coupling to such possible states should be much weaker, and the lifetime much longer than the $\sim 10^{-10}$ sec observed for decay into two π mesons. In sum, the existence of a neutral K meson was predicted to be produced in equal abundance with the known K_1^0, sharing its static properties, but whose decay rate was much slower and decay modes anomalous (i.e., $\not\rightarrow \pi^+ + \pi^-$). On the basis of these considerations the experimental search for a long-lived neutral K-meson was undertaken.

The later discovery that parity and charge conjugation were not conserved in $\pi \rightarrow \mu$ and β decay (*2*) and the consequent strong suspicion that these conservation laws were also invalid in the K^0 decay, rendered the arguments in the form given by Pais and Gell-Mann invalid. As was shown by Lee, Oehme, and Yang (*3*) however, this particle mixture description of the neutral K meson follows rather from more general quantum mechanical considerations. The conservation laws serve to fix the amplitude and relative phase of the two components of the mixture. We may consider the situation by noting that the reactions

$$K^- + P \rightarrow N + K^0 \rightarrow N + [\pi^+ + \pi^- + 214 \text{ Mev}],$$
$$K^+ + N \rightarrow P + K^0 \rightarrow P + [\pi^+ + \pi^- + 214 \text{ Mev}]$$

are both known (*4*, *5*) to occur. There is ample evidence for the assignment of opposite strangeness to K^+ and K^- and to the conservation of strangeness in these strong reactions. In both reactions the subsequent decays of the neutral K-mesons are identical. It follows that each neutral K must be described as a mixture of K^0 and the charge conjugate $\bar{K}^0$, whose strangeness is uniquely defined only at the time of production. The two mixtures would not in general have the same mean lives. Without appealing to the conservation laws the amplitudes of the K^0 and $\bar{K}^0$ fields and their relative phase in the mixtures K_1^0 and K_2^0 cannot be uniquely determined and the relative decay rates cannot be specified. There are however, two possible situations where a large difference in lifetime would be predicted and indeed the observable consequences would be very similar to those discussed by Pais and Gell-Mann. First, if time reversal is rigor-

ously conserved in the decay the arguments above carry through with the charge conjugation operator everywhere replaced by the mixed parity (CP) operator (*6*, *7*). Further, if for some extraneous reason, such as the availability of phase space, those matrix elements which couple to a particular final state (e.g., $\pi^+ + \pi^-$) were dominant, the situation would be essentially independent of whether any of the conservation laws, charge conjugation, parity or time reversal, were valid (*3*). Again one would predict the existence of a neutral K meson of long lifetime with decay into $\pi^+ + \pi^-$ essentially forbidden.

The significance of the existence of *two* final decay states, $\pi^+ + \pi^-$ and $\pi^0 + \pi^0$, with comparable rates (*8*) has recently been emphasized by Weinberg (*9*). Lacking some special phase relation between these two modes, a large difference in the decay rates of the two mixtures would not be expected. Time reversal invariance would fix the relative phase in just such a way, as is mentioned above. With this view, observation of a long-lived neutral K meson for which 2 pion decay is forbidden would be evidence for time reversal invariance in the decay interaction.[1]

At the time these ideas were first introduced, relevant data were very meager. Both in the cosmic ray experiments [see data reviewed by Thompson (*10*)] and the early work on strange particle production in complex nuclei (*12*) at the Brookhaven Cosmotron the observed ratio of Λ^0 to θ^0 decays was roughly 3 to 1, even with possible Λ^0, K^+ production eliminated (*12*). An abundance of possibilities was available to explain this deviation from the value unity predicted by associated production theories. It could not be inferred that a long-lived and therefore undetectable K^0 was produced in association with a Λ^0 in some fraction of the events. Some examples of anomalous K^0 meson decays had been observed,[2] but it was not then clear that these were not alternate decays of the short-lived K_1^0.

An experimental program to detect and identify long-lived neutral K particles and investigate the characteristics of their decay was then undertaken. The results, indicating the existence of such particles and describing some properties have been reported in part earlier (*14*). We present here a final summary of the results in greater detail.

II. EXPERIMENTAL ARRANGEMENT

A. Geometry

The detector, the Columbia 36-in. diameter expansion cloud chamber, was exposed to the secondary neutral radiation produced by 3-Bev protons in a copper

[1] Recent experimental results indicate the selection rule $\Delta T' = \frac{1}{2}$ in the K^0 decay may be valid. This would also fix the relative phase of the two modes and account for a large difference in lifetime. In such case no evidence for time reversal invariance is obtained (*11*).

[2] Cosmic-ray data are summarized in Ballam *et al.* (*13*). However, see also other works cited in Ref. *13*.

target. Discrimination against well-known V^0 decays is assured with the target to chamber distance long compared to the mean flight paths of the known particles produced at this energy. Exposures were made at two distances so that the K_2^0 lifetime could be determined from a comparison of the yields. To maximize the yield in the short-distance run, the target to chamber distance was the minimum obtainable with the arrangement used.

The distances from the target to the cloud chamber entrance wall were 16-ft. and 70-ft., corresponding to mean flight times 2×10^{-8} sec and 8.4×10^{-8} sec. A plan view of the arrangements is shown in Fig. 1. For the short distance run the 3-Bev proton beam was extracted from the Cosmotron, focussed by a pair of 12-in. diameter quadrupole magnets, deflected twice in magnets of 18-in. by 36-in. pole area and deposited on a copper target $1\frac{1}{2} \times 6$-in. in cross section and 4-in. long. A beam at 68° to the direction of incident protons, of solid angle 0.002 stearad, was defined by the $1\frac{1}{2}$ in. $\times$ 5-in. aperture in the 4-ft. thick lead shielding wall. Charged particles were eliminated from this secondary beam by the combination of the collimating slit and the following 4×10^5 gauss-in sweeping field. Since the target is also an intense source of high energy gamma rays, a 1.5-in. thick lead filter was interposed at the collimator entrance.

An increase in target to chamber distance, required for purposes of lifetime measurement, could not be conveniently provided using this general arrangement and keeping the 68° viewing angle constant. Instead, the longer distance was achieved by placing a target in a curved sector of the Cosmotron at an azimuth such that the flight path to the chamber made an angle of 68° $\pm$ 1° to the circulating beam. With this arrangement the Cosmotron guide field removed

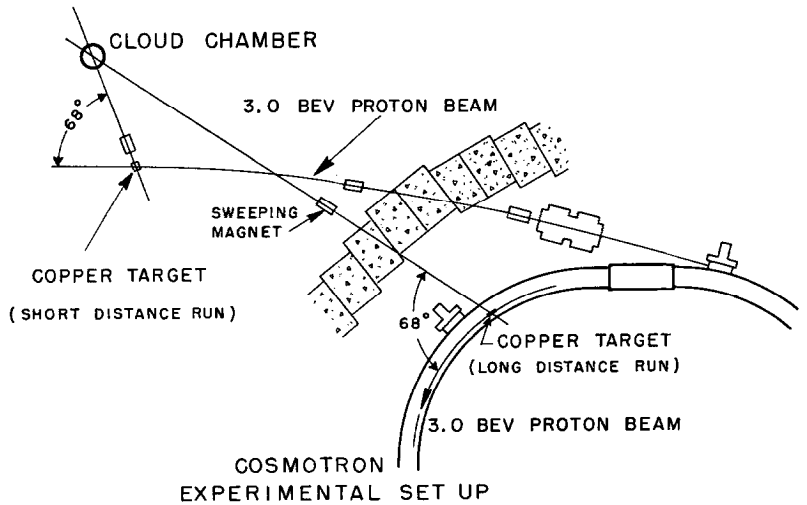

FIG. 1. Experimental arrangement, showing disposition of the beams in both the long and short distance exposures.

charged particles from the secondary beam. The direction was defined by an 8-ft. long, 1½-in. by 7-in. aperture iron collimator inserted into the main shielding wall. The collimator slit limited the beam to ~3-in. by 18-in. at the chamber entrance. A 4×10^5 gauss-in. magnet following the collimator removed charged particles produced by the beam after leaving the Cosmotron magnetic field. At some 20-ft. from the chamber an 8-ft. thick concrete wall was erected to shield from general background radiation. The aperture here, 18-in. × 18-in. was large enough to prevent the production of secondaries by the neutral beam particles. Again a 1½-in. thick lead absorber located near the Cosmotron vacuum chamber removed γ-rays.

B. Beam Monitoring

At the target position the external proton beam envelope was roughly circular in cross section with 2½-in. diameter at half maximum intensity. The shape and location of the beam was determined from induced activity distributions in Al foils periodically exposed to the full proton beam. Standard radiochemical techniques were used.[3] With 10^7 protons per millisecond in such an area, electronic counting techniques cannot be used. Relative intensities were determined from the time-integrated voltage output pulse from a 2-in. diameter, 2-in. thick water Čerenkov counter in the proton beam. This counter served also to monitor the beam position and to time the cloud chamber cycle. The Čerenkov counter was calibrated by comparison of the time average output pulse height with the induced radioactivity in a 0.016-in. copper foil exposed during a part of the run. In particular the β decay rate of Mn^{52} produced during the bombardment was measured. This method suffers from several sources of inaccuracy. The cross section for production of Mn^{52} by 3-Bev protons is known to ±10% (*15*). Fluctuations in the position and shape of the beam, due to variations in magnet currents change the correspondence between counter output and foil radioactivity; the influence of secondary particles scattered from the target into the foil is not understood. We estimate then the average proton beam on the target to have been $6 \pm 2 \times 10^7$ protons per pulse. This intensity was limited by the number of neutron recoils and slow electrons in the chamber.

Induction pickup electrodes measured the circulating beam intensity, during the long distance exposure, to an estimated accuracy ±20%. The internal copper target was 1-in. vertically by ½-in. horizontally and 2-in. along the beam direction. As is usual a thin copper projecting lip on the target served to damp betatron oscillations and accelerate the inward motion of the beam. The presence of the lip does not affect the correspondence between circulating intensity and number of protons on the target, but increases the effective target length. The

[3] We are indebted to G. Friedlander, J. Cumming, and others of the Brookhaven National Laboratories Chemistry Department for these measurements.

transverse dimensions of the target are sufficiently large to permit the assumption that all circulating protons strike the target. In the long distance exposure we estimate then an average intensity $11 \pm 3 \times 10^8$ protons per pulse. For equal intensity of neutrons traversing the cloud chamber in the two exposures, taking account of the solid angles and target thicknesses, one would have expected a ratio of beam intensities 0.10, consistent with the observed 0.06.

C. Cloud Chamber and Photograph Analysis

Decays of V particles were observed in a conventionally designed expansion cloud chamber 36-in. in diameter and illuminated over an 8-in. depth. It is operated at an 80-sec repetition rate. The chamber is in a magnetic field of 10,000 gauss, uniform to $\pm 2\%$ over the illuminated volume. Details of the chamber operation have been published elsewhere (*16*). To minimize the number of neutron interactions the chamber was operated at a pressure of 0.81 atmos helium plus 0.20 atmos argon, the lightest gas mixture usable, consistent with good chamber operation. Further, the lucite entrance wall of the chamber was reduced to $\frac{1}{16}$-in. thickness over an area of 3-in. $\times$ 18-in. These measures were designed to reduce the already small density of the large detector volume. As a result readable photographs were obtained with an estimated flux of $\sim 10^4$ neutrons per pulse. At this rate, an average of two neutron stars in the gas per picture was observed. The background limiting the usable proton beam intensity to $\sim 1\%$ of that available consisted of 50–100 protons ejected from the chamber wall by the beam neutrons.

Photographs were taken in three cameras arranged with their lens axes parallel and in a line. For scanning and measurement each of the three views is projected at half scale. A representative picture is shown in Fig. 2. Techniques of searching for possible V particle decays included: following all tracks of negatively charged particles to possible intersection with a positive track; area scanning to find such vertices; following all tracks of near minimum ionization to a possible vertex. All such vertices are recorded as are evident neutron induced stars of two or more prongs.

In each of the three views the radius of curvature of each track of a "V" is measured by fitting to a template. For very short tracks, the coordinates of the droplets were measured directly on the film using a traveling stage microscope. A least squares fit was made to a parabola (*17*) to determine the radius of curvature. Dip angles and the projected angles with respect to the incoming beam direction are measured in the reprojected image. The direction of the beam in the cloud chamber fiduciary system was determined from measurements on incoming charged particles in pictures obtained with the sweeping magnet and cloud chamber magnet turned off. Corrections for conical reprojection were made with the series expansion discussed by Sargent *et al.* (*18*).

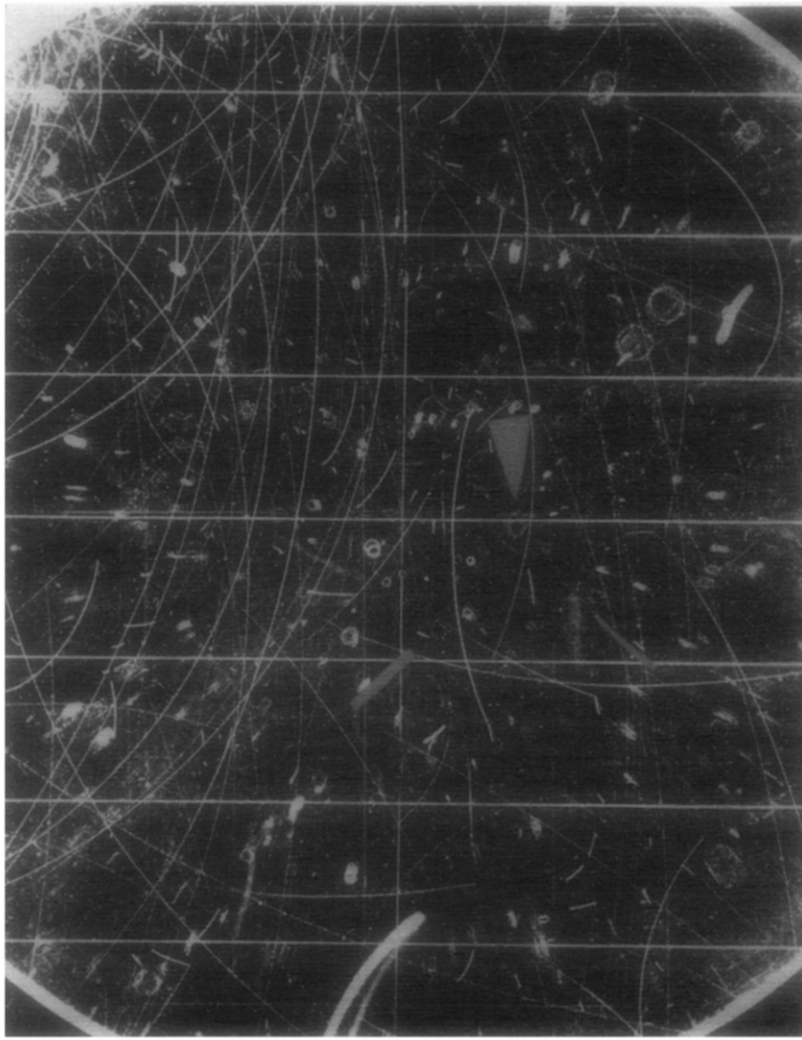

FIG. 2. An example of a K_2^0 decay, showing most of the chamber volume. The point of decay of the K_2^0 is indicated by the arrowhead.

Momenta were generally in the range 50 Mev/c — 300 Mev/c and were measured with an estimated accuracy, on the average $\pm 10\%$. Angles were measured to an accuracy $\pm \frac{1}{2}°$ in the horizontal plane and $\pm 3°$ in the vertical plane.

To determine masses of the decay products, where identifications could successfully be made, ionizations greater than minimum were determined by photo-

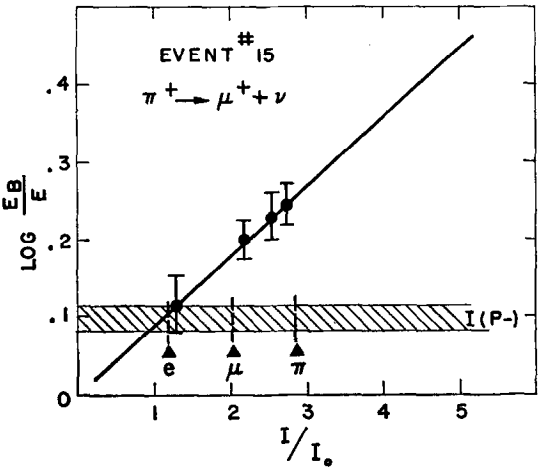

FIG. 3. Ionization calibration curve. The points on the curve indicate the density o nearby proton tracks of known ionization. The vertical dashed lines represent the ioniza tion of the negative secondary if it is a π, μ or electron. The shaded region shows the uncertainty in the absorption measurement.

metric analysis using techniques similar to those described by Caldwell and Pal (*19*). A fine slit 1 cm long is oriented along the track and driven across the track by a synchronous motor which is also coupled to a galvanometer. The slit is then translated parallel to the track and the traversal repeated for as long as the track is in view. The ratio of peak density to background density is averaged for the track and the log of the result is entered on a calibration plot obtained by repeating this procedure for all the protons in the same photograph which pass near the event of interest, within ± 5 cm of the height of the event and which have dip angles of less than 20°. An uncertainty is assigned to each result which is based on the average deviation of the various readings from the mean. Mass identification is said to be made when the result is established to a confidence level $\sim 80\%$, treating the uncertainties as standard deviations. In practice only tracks with momenta $\lesssim 100$ Mev/c were identified. Figures 3 and 4 illustrate the identification of secondaries by this technique.

III. RESULTS—SHORT DISTANCE EXPOSURE

A total of 6500 pictures was taken in the short distance run. These yielded 152 examples of V^0 decays. Among the charged secondaries pions, muons and electrons, were identified, but no K-mass or heavier particles were found. All the events but one were noncoplanar with the line-of-flight to target or showed nonzero transverse momentum. The distribution of vertices was uniform over the chamber, indicating a lifetime $\gg 10^{-9}$ sec. In the same sample, we found 9369 neutron induced stars of ≥ 2 prongs in the gas, 586 electron-positron pairs

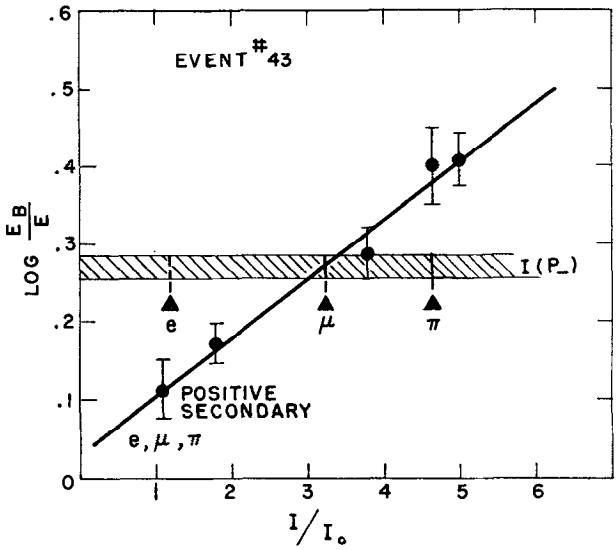

FIG. 4. An ionization measurement showing an identified negative muon.

(by definition: $\sim 0°$ opening angle between minimum ionizing tracks) and 402 events which were consistent with π-μ decay kinematics.

IV. BACKGROUND

Since our major effort was toward the establishment of the existence of a long-lived K^0 particle, we will here consider in some detail the possibility that the observed events are rather background events which simulate K^0 particle decays.

The major background effects which could simulate V particle decays are meson pair production in the cloud chamber gas, pion scattering, electron pairs from internal or external conversion of γ rays and electron radiative scattering.

A. Meson Pair Production

In the collisions of a 3-Bev proton with a target neutron of 25-Mev Fermi energy, neutrons at 68° to the proton direction have a maximum energy of 470 Mev. Double meson production at this energy is essentially nonexistent. In fact, however, a small fraction of the neutrons in the beam were of greater energy. The energy spectrum of protons ejected from the chamber wall in a direction parallel to the incident neutrons is shown in Fig. 5. The threshold energy for production of pion pairs by nucleons on complex nuclei is $\sim$360 Mev. The proton spectrum (Fig. 5) indicates that the neutron energy distribution was approximately uniform from this threshold energy to $\sim$900 Mev.

Of 9369 stars observed, 15 had a negative π meson prong. To permit an esti-

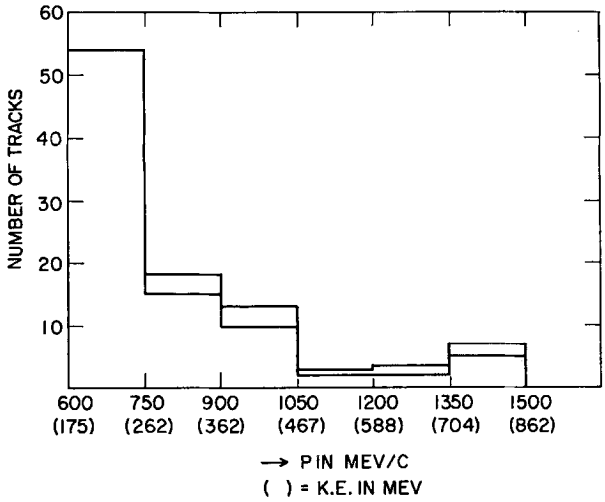

FIG. 5. The lower histogram is the spectrum of protons ejected from the entrance wall by neutrons in the direction of the incoming K_2^0 beam. The upper histogram shows the incoming neutron energy spectrum obtained from the proton spectrum by use of the N-P cross section.

mate of the double meson production, we assume these are examples of single meson production and that they are produced by neutrons of energy greater than the double meson production threshold. Further, we assume the energy dependence of the cross section on complex nuclei to be the same as that in free nucleon-nucleon interactions over the corresponding energy range, 600 Mev to 1300 Mev. Note that charge symmetry requires equal cross sections for the reactions $N + N \rightarrow \pi^- + N + P$ and $P + P \rightarrow \pi^+ + N + P$ and for $\pi^+ \pi^-$ production. For incident proton energies in the range 600 Mev–1000 Mev the experimental data are consistent with zero cross section for double meson production in P-P collisions.[4] The average cross section for single π^+ production over this energy range is 18 mb (*20*). Above 1-Bev bombarding energy the π^+ production cross section is $\simeq$25 mb, the π^+ π^- cross section is $\simeq$5 mb . The inelastic N-P cross section shows approximately the same energy dependence, and is roughly 60% of the P-P inelastic cross section.[5] Wallenmeyer (*22*) observed, in N-P collisions below 1-Bev incident energy, a $\pi^+ + \pi^-$ to single π^- production ratio $\simeq$0.2. Above 1-Bev double meson production dominates, with the ratio of single to double production

$$\sigma_{NP}{}^{\pi^-} : \sigma_{NP}{}^{\pi^-\pi^0} : \sigma_{NP}{}^{\pi^+\pi^-} = 46:14:62.$$

[4] A summary of available data on meson production in P-P collisions is given by Lock (*20*).

[5] These data are summarized by Riddiford (*21*).

For our purposes the $\pi^- \pi^0$ production is included with the single π^- production. An overestimate of the absolute cross section for double production results from our neglect of π^0 creation. In N-P collisions below 1 Bev then

$$\sigma_{NP}{}^{\pi^-} = 8 \text{ mb}, \qquad \sigma_{NP}{}^{\pi^+\pi^-} = 2 \text{ mb}$$

and above 1 Bev

$$\sigma_{NP}{}^{\pi^-} + \sigma_{NP}{}^{\pi^-\pi^0} \cong \sigma_{NP}{}^{\pi^+\pi^-} = 9 \text{ mb}.$$

The cross sections for single meson and pair creation in N-N collisions are those given above for P-P interactions. With the assumed uniform neutron energy distribution, the ratio of $\pi^+ + \pi^-$ to π^- production in the neutron interactions in the cloud chamber gas is

$$\frac{N(\pi^+ + \pi^-)}{N(\pi^-)} = \{\tfrac{4}{7}(\sigma_{NP}{}^{\pi^+\pi^-})_{<1 \text{ Bev}} + \tfrac{3}{7}[(\sigma_{NP}{}^{\pi^+\pi^-})_{>1 \text{ Bev}} + (\sigma_{NN}{}^{\pi^+\pi^-})_{>1 \text{ Bev}}]\} \div \{\tfrac{4}{7}[(\sigma_{NP}{}^{\pi^-})_{<1 \text{ Bev}} + (\sigma_{NN}{}^{\pi^-})_{<1 \text{ Bev}}] + \tfrac{3}{7}[(\sigma_{NP}{}^{\pi^-})_{>1 \text{ Bev}} + (\sigma_{NP}{}^{\pi^-\pi^0})_{>1 \text{ Bev}} + (\sigma_{NN}{}^{\pi^-})_{>1 \text{ Bev}}]\} = 0.23.$$

Any reabsorption of pions within the nucleus would lead to a smaller ratio. In our sample of neutron stars there should have been less than 4 cases of production of a pair of charged pions. One such star was indeed found. Difficulty in distinguishing positive pions from protons precludes the possibility of an estimate of the total pion pair production. To simulate a V^0 decay, however, the nucleon recoil prongs would have to be invisible, i.e., proton energies <1 Mev. We conclude then that neutron-produced pion pairs at most constitute 1 % of those V's interpreted as $K_2{}^0$ decays.

B. Pion Scattering

Some fraction of the pions produced in a backward direction by neutrons in the rear wall of the chamber will scatter in the gas without a visible recoil, producing spurious V^0 decays. The flux of pions is determined from the number of $\pi \rightarrow \mu$ decays, those being consistent with the pion decay kinematics. The average pion energy was 65 Mev, the total path length was 59 g/cm^2 of He plus 132 g/cm^2 Argon. Fowler *et al.* (*23*) measure a mean free path in helium of the order of 50 g/cm^2 for pions of this energy. Thus one scattering from helium is expected. In argon the interaction cross section is geometric and again one scattering is expected. The flux count must be multiplied by a correction factor, estimated to be 2–3, to take into account the inefficiency in detecting π-μ decays at small angles. We estimate then 4–5 pion scatters to have occurred. This number is greatly reduced when one considers that the recoil must not be visible. Pion scatters then do not contribute significantly to the $K_2{}^0$ decay events.

This conclusion is reinforced by kinematical considerations. On the assumption that each V^0 is an elastic pion scattering, we have determined the mass of the recoil particle. In each case this mass was less than the nucleon mass. None of the events can then be an elastic scattering. It is known that at these energies greater than 50% of pion interactions with nuclei are elastic. It is then unlikely that there is any contamination of pion scatters in the sample of V^0 decays.

C. Alternate Mode of π^0 Decay

Electron-positron pairs produced in the internal conversion of π^0 decay γ-rays have larger mean opening angle than those externally converted. These were therefore considered the more serious possible contribution to spurious V^0 decays. Note that to be confused with a genuine decay it is necessary that the π^0 be produced in the gas without visible nuclear recoil.

The arguments detailed in (A) above apply here also. Rates of neutral pion production (*20*) in N-N collisions are smaller than charged pion rates by factors of 3–10 over the energy range considered here. It can be shown, using requirements of charge independence, and measured cross sections (*20–22*) for other pion production reactions, that π^0 production cross sections in N-P collisions are larger, by 10 mb on the average, than the charged pion production cross sections. In fact, the π^0 creation accounts for greater than 60% of the inelastic cross section. Let us assume that π^0's are produced in all inelastic N-P interactions, with average cross section 10 mbn; in N-N collisions with 3-mb cross section. Negative pion production cross sections, with these assumptions are $\sim$20 mb. The ratio of π^0/π^- production in complex nuclei is then $\sim$0.7. Accompanying the 15 observed π^- productions should be $\sim$10 π^0's. Only one π^0 in 80 decays via the $e^+e^-\gamma$ mode. This makes it extremely improbable that any of the presumed K_2^0 decays are such electron-positron pairs.

Kinematic arguments are applied here also. Each event was assumed to be an electron-positron pair and an apparent Q value calculated in the usual way.[6] The observed distribution is shown in Fig. 6. Any V with a Q value greater than the π^0 mass, 135 Mev, cannot have been a π^0-decay product. In this way, all but 30 events are shown to be something other than π^0-decay pairs.

D. Electron Pairs

The events classified as unstable particle decays all had apparent Q values greater than 20 Mev, on the assumption that they are rather electron pairs. The distribution in Q value, calculated by Borsellino (*25*) shows a Q^{-3} dependence for values greater than $\sim$2 Mev and is approximately independent of the

[6] Peyrou (*24*) pointed out that consideration of the apparent Q value is most convenient to discuss these electron pairs.

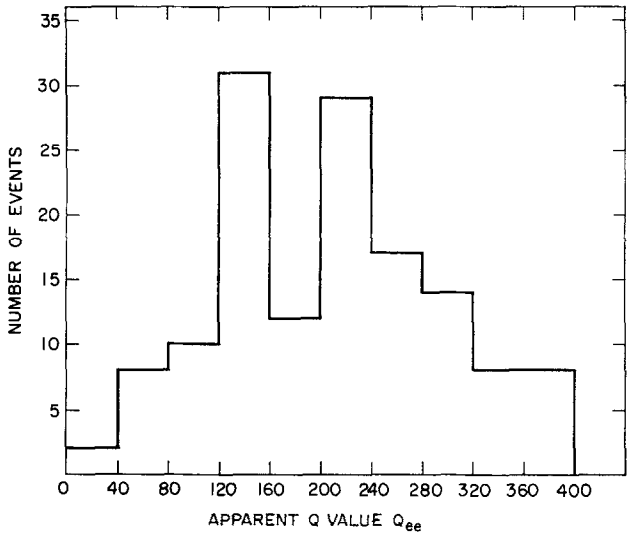

FIG. 6. The distribution of apparent Q_{ee} value, on the assumption that each event is an electron-positron pair.

γ-ray energy. The probability that an electron-pair have $Q > 20$ Mev is $<1\%$, and $<0.1\%$ will have $Q > 60$ Mev. As seen in Fig. 6, two events had $20 \leq Q \leq 40$ Mev and one had $40 \leq Q \leq 60$. This is to be compared with 586 events, with $\sim 0°$ opening angle, which were classified as converted γ-rays. At most the three events indicated could represent an electron pair contamination in the K_2^0 sample.

E. Bremsstrahlung

Backward-going electrons can result from internally or externally converted photons from decay of neutral pions produced in the cloud chamber wall. From arguments above (A, C) it is estimated that this flux can at most amount to a few percent of the charged pion background. It was concluded in (B) that only 4–5 pion scatters could have occurred. It is then clear already that scattered electron contamination is negligible.

Detailed angular distributions of electron radiative scattering have been given by McCormick *et al.* (*26*). The largest opening angle of any of the events here was 145°, with the distribution shown in Fig. 7. This fact eliminates the possibility of any of the V^0 events being π-μ decays, since the maximum angle in this case is $\sim 20°$ for all but extremely low energy pions. The probability that an electron be deflected through greater than 30° is less than 1% at an electron energy of the order of 100 Mev. It is unlikely that any of the events is the result of electron bremsstrahlung.

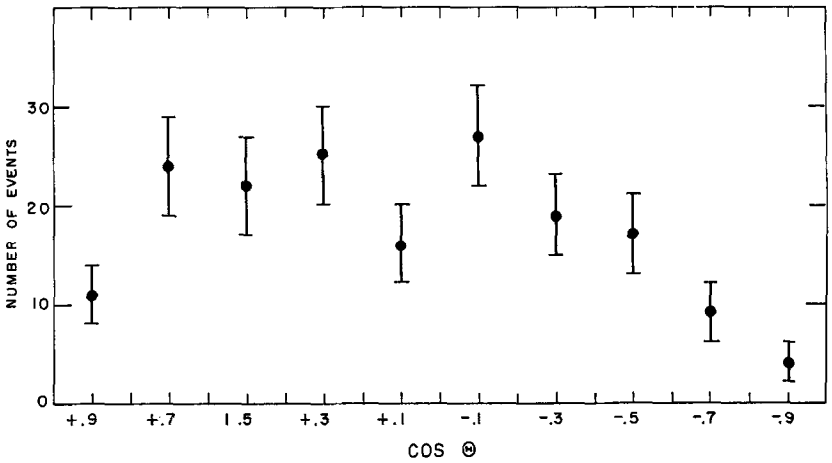

FIG. 7. The distribution in opening angle for all events observed in the short-distance exposure.

Consideration of these most likely sources of background leads to the conservative conclusion that all but perhaps three or four of the V events observed and classified as unstable particle decays are genuine examples of such decays.

It seems natural and economical to assign this neutral unstable particle to the K_2^0 level in the Gell-Mann, Nishijima scheme, especially in view of the bubble chamber observations that just half of the θ^0's produced in $\pi^- + P$ collisions are accompanied by observed K_1^0 disintegrations (*27*).

V. ANALYSIS OF EVENTS—PROPERTIES OF THE K_2^0

A. MASS

It is not in general possible to uniquely determine the mass of the parent particle from the measurements of the secondary tracks. Kinematic analysis yields a mass determination only in the case of two body decay. We resort to less direct arguments to establish limits on the mass of the particles observed.

In Fig. 8 we plot the distribution of transverse momentum of the positive, negative and neutral (only one is assumed) decay products. The transverse momenta of the charged particles are directly measured, that of the neutral particle inferred from transverse momentum balance. This distribution is of course independent of any secondary mass assignments. The measured maximum transverse momentum is 230 $\pm$ 20 Mev, determined by folding momentum resolution into a linear spectrum near the upper end point. The decay product of mass m_1, from the decay of a particle of mass M will have a maximum transverse momentum

$$\bar{P} = \frac{[M^2 - (m_1 + m_2 + m_3)^2]^{1/2}[M^2 - (m_1 - m_2 - m_3)^2]^{1/2}}{2M},$$

where m_2 and m_3 are the masses of the other secondaries. Solving for M as a function of m_1, m_2, m_3, we find the limits

$$460 < M < 630 \text{ Mev}$$

consistent with the θ_1^0 mass of 494 Mev.

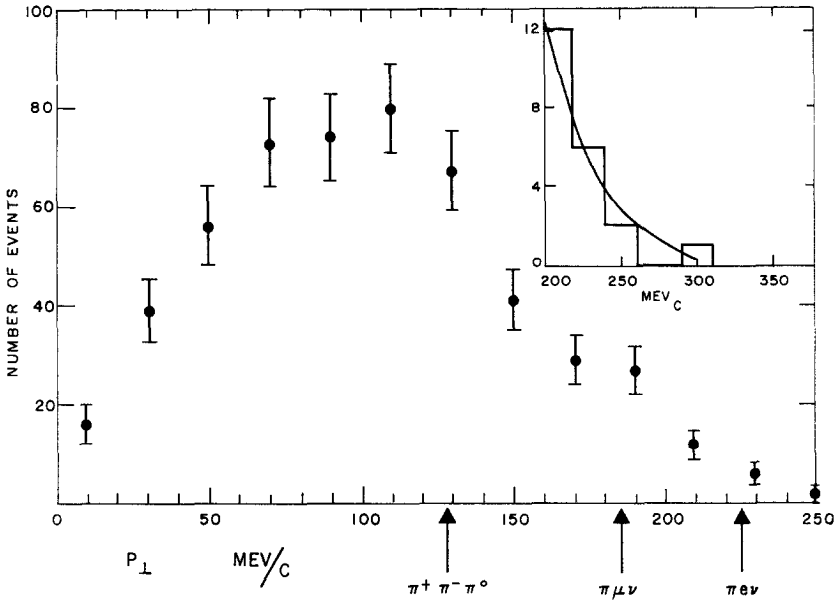

FIG. 8. Transverse momenta of the positive, negative and neutral secondaries of the short-distance events. The arrows show maximum values for the decay modes indicated. The inset compares the distribution near the end point with a resolution-folded linear cut-off at 230 Mev/c.

The possibility that these could be decays of hyperons via the modes $N + \mu^{\pm} + e^{\mp}$ or $N + e^+ + e^-$ was also considered. It should be noted first that no examples of a corresponding decay into a proton plus two leptons were observed. Each event was analysed on the assumption of such decay schemes. In no case was the apparent Q value consistent with the known Λ^0 or Σ^0 mass, and these data do not justify the assumption of a new hyperon.

B. Decay Modes

All the events reported here are kinematically consistent with the decay of a K-mass particle into one or more possible three body final states. Guided by the known decay schemes of the K^+ we assume that only the corresponding modes

$\pi^{\pm}\mu^{\mp}\nu$, $\pi^{\pm}e^{\mp}\nu$ and $\pi^{+}\pi^{-}\pi^{0}$ are permitted. The three pion mode is considered more probably than the $\pi^{+}\pi^{-}\gamma$ for theoretical reasons given by Dalitz (*28*).

It is possible to kinematically distinguish among these possibilities in some cases, even though the K_2^0 velocity is unknown. Since it may be of general interest, we shall discuss in some detail the kinematics of the three body decays.

The measured quantities are the secondary momenta P^{+}, P^{-}, the opening angle θ and the angles of the secondary momenta to the primary line of flight β^{+} and β^{-}. With these we calculate the total visible momentum P_T and its angle to the beam direction β_T. A particular set of secondary masses m_+, m_-, m_0 is assigned. It is convenient to define a fictitious mass

$$M_T = (E_T^2 - P_T^2)^{1/2},$$

where E_T = total visible energy. The apparent Q value for the particular decay scheme is

$$Q_{m+m-} = M_T - (m_+ + m_-),$$

which must be less than the true Q value

$$Q = M_K - (m_+ + m_- + m_0).$$

For any given event, those secondary mass assignments which lead to apparent Q values greater than the true Q value are eliminated as possibilities.

The energy of the neutral secondary in the rest system is uniquely determined

$$E_0 = \frac{M_K^2 + m_0^2 - M_T^2}{2M_K}$$

as is its angle, in the rest system, to the K^0 line of flight

$$\sin \bar{\beta}_0 = \frac{P_T \sin \beta_T}{P_0}.$$

In general it cannot be determined whether the neutral particle goes forward or back in the center-of-mass system. Thus the energy of the parent K meson has two possible values.

The magnitude of the neutral secondary momentum in the rest system, $\bar{P}_0$ is independent of the angle β_T. Another kinematic criterion is thus provided by the requirement that there be zero momentum in the center of mass. Those decay mode assignments which do not satisfy the requirement,

$$P_T \sin \beta_T \leq \bar{P}_0$$

are eliminated from consideration in each case. Further, if the measurements yield $P_T < \bar{P}_0$ then $P_T < \bar{P}_T$ and $\bar{P}_0$ must then be forward. In such cases the ambiguity in the energy of the K_2^0 is removed.

A further kinematic criterion is that the transverse momentum of each of the decay products be less than the maximum center of mass momentum for that particular mode.

Applying these criteria, we find of the 152 (short distance) events 10 events consistent only with $\pi^+e^-\nu$, 5 cases of $\pi^-e^+\nu$ and 12 satisfying either $\pi^+e^-\nu$ or $\pi^-e^+\nu$. Further the low Q value for the $\pi^+\pi^-\pi^0$ mode allows us to rule out all but 23 cases as possible τ^0 events.

Unique identifications were also obtained with ionization and momentum measurements of the secondary tracks. See Figs. 3 and 4. In four cases both secondary masses were identified, one each of π^+e^-, π^-e^+, $\pi^+\mu^-$, and $\pi^-\mu^+$. Others for which one secondary was identified included 4 examples of π^+e^-, 1 or π^-e^+, 9 of $\pi^+\mu^-$, and 1 of $\pi^-\mu^+$. The ionization-identified π^+e^- cases were kinematically consistent only with this decay scheme, as was one case of π^-e^+. In one of these the electron was accompanied by a $\pi^+ \rightarrow \mu^+$ decay. Two examples of the τ^0 mode ($\pi^+\pi^-$) have been previously reported (*14*).

In total, of the sample of 152 K_2^0 decays, we identify 10 $\pi^+e^-\nu$, 6 $\pi^-e^+\nu$, 12 $\pi^\pm e^\mp\nu$, 10 $\pi^+\mu^-\nu$, 2 $\pi^-\mu^+\nu$, and 2 $\pi^+\pi^-\pi^0$. Here the neutral particle is assigned on the basis of the known K^+ decay modes.

Further identification of single secondaries were: 5 π^- and 3 π^+ from ionization measurements; 1 $\pi^+ \rightarrow \mu^+$ and 1 $\pi^- \rightarrow \mu^-$ decay. These identifications are summarized in Table I. Strong bias operates in the identifications of the π's, μ's, and e's. Consequently very little is known of the ratio of $\pi\mu\nu$ to $\pi e\nu$ except that both are prominent. Also the τ^0 mode is present to $\lesssim 15\%$.

No decays were found which did not fit one of the assumed modes $\pi^\pm e^\mp\nu$, $\pi^\mp\mu^\pm\nu$, or $\pi^+\pi^-\pi^0$. Of course nothing can be said about the existence of such modes as μ^+e^- + neutral, etc. Observation of five $\pi \rightarrow \mu$ decays among the V^0 secondaries is consistent with $\sim$100 charged pions among the decay products.

The total number of events observed in both runs was 186. Of these, only two had zero total transverse momentum within the errors. One of these is noncoplanar with the K_2^0 line of flight and the other has a very low $Q_{\pi\pi}$ value. Thus none of the 186 events can be a two body decay of the K_2^0 and we can

TABLE I

SUMMARY OF IDENTIFIED DECAY SCHEMES

	$\pi^+e^-\nu$	$\pi^-e^+\nu$	$\pi^+\mu^-\nu$	$\pi^-\mu^+\nu$	$\pi^+\pi^-\pi^0$
Both secondaries identified by ionization	1	1	1	1	
Lepton only identified by ionization	3	1	9	1	
Ionization identification plus $\pi \rightarrow \mu$ decay	1				2
Kinematical determination	5	4			
Total	10	6	10	2	2

set an upper limit $<0.6\%$ on the reactions

$$K_2^0 \rightarrow \begin{cases} \mu^{\pm} + e^{\mp} \\ e^+ + e^- \\ \mu^+ + \mu^- \end{cases}$$

and on $K_2^0 \rightarrow \pi^+ + \pi^-$.

The absence of two body leptonic modes is consistent with the predictions of the universal Fermi interaction since these modes cannot be directly generated by the currents which account for β decay and μ decay. The absence of the two pion final state is consistent with the predictions of time reversal invariance as discussed earlier.

VI. LIFETIME

A. Experimental Results

The uniform distribution of decay points of the 152 K_2^0's served to put a lower limit in the mean life $> 4 \times 10^{-9}$ sec. Analysis of anomalous V^0 decays observed in cosmic ray experiments gave lifetime estimates $\tau > 6 \times 10^{-9}$ sec. from Kadyk *et al.* (*29*), and from the Ecole Polytechnique group: $\tau \lesssim 10^{-7}$ sec (*30*). Lack of anomalous K^0 decays near production points in bubble chambers had served to set a limit $\tau > 3 \times 10^{-8}$ sec (*8*). The time of flight of the K_2^0 in a typical detector is then small compared to the mean life. In this case, the lifetime is best determined by comparing the yields with the detector at different distances from the production target, corresponding to times of flight to the detector differing by a time at least of the same order as the lifetime.

The mean times of flight to the chamber in the two exposures were 2×10^{-8} sec and 8.4×10^{-8} sec. As discussed above, proton flux determinations are intrinsically inaccurate and difficult to interpret because of the differences in the geometry of the two arrangements. To normalize the K_2^0 flux in the two exposures we used the observed number of neutron induced stars in the cloud chamber gas. The energies of neutrons emitted near 68° are quite sensitive to the angle of emission. To check that the production angle of the K_2^0 beam was the same in each run, and to be certain that the neutron background came directly from the target, three independent determinations of the neutron energy spectra were made.

(1) The distribution in number of star prongs in the two runs is compared in Fig. 9.

(2) The momentum spectra of protons ejected in the forward direction ($\pm 5°$) from the lucite entrance window are compared in Fig. 10.

(3) The momentum distribution of the star prongs is compared in Fig. 11.

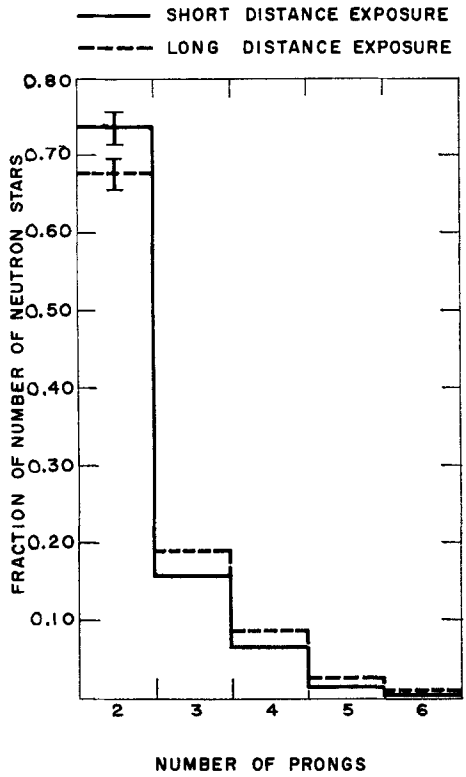

FIG. 9. Prong distributions of neutron induced stars in the cloud chamber gas.

The results of the first two checks indicate identical spectra of neutrons incident upon the chamber. The small discrepancy in percentage of two-prong stars is precisely accounted for by the slightly higher fraction in the long distance run of argon in the He-A mixture of the cloud chamber gas. The third comparison is made to insure that the neutrons inducing the stars come *directly* from the target in both runs. A contamination of stars produced by neutrons diffusing through shielding walls could confuse the relative flux determination. The results show no evidence for this effect which would predict a larger number of low energy prongs in the short distance exposure.

In the short-distance exposure, we counted 152 K_2^0-decays and 9369 neutron stars of two or more prongs; in the long-distance exposure 34 K_2^0-decays were found in 4887 neutron stars. The ratio of the yields in the two exposures is then: $R = 0.43 \pm 0.08$. A correction must be made for the slightly higher proportion of Argon in the second run, giving rise to an increased cross-section for star production.

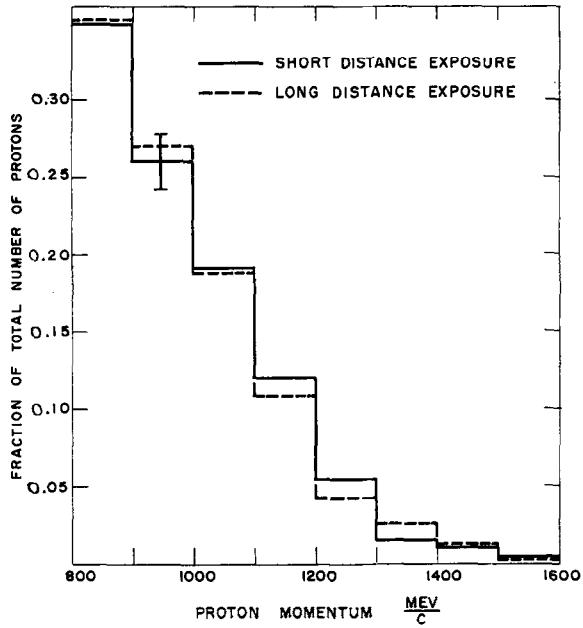

FIG. 10. Momentum distributions of protons ejected from the entrance wall by neutrons.

To compute a lifetime, two additional factors must be considered: (1) the relative scanning efficiency, and (2) the velocity distribution of K_2^0-particles. Second, third, and, in a fraction of the data, fourth scanning indicate a scanning efficiency in the first run of (85 $\pm$ 10) % the efficiency in the second run. Some additional checks were made. The events and stars occurring in the central 5 cm of the 20-cm chamber depth were selected. In this region the illumination is >70 % of the peak illumination. This restriction leads to a ratio: $R = 0.45$ and indicates that a lower efficiency in observing "faint" events is not a serious source of error. Also, normalization made on stars of 3 or more prongs gives a similarly consistent result. Combining the relative scanning efficiency of 0.85 $\pm$ 0.10, we then have:

$$R = 0.41 \pm 0.10. \tag{1}$$

This ratio is given as a function of τ, the mean life of the K_2^0 by:

$$R = \frac{\int P(\beta\gamma) \exp\left[-t_L(\beta\gamma)/\tau\right]\{1 - \exp\left[\Delta t(\beta\gamma)/\tau\right]\} d(\beta\gamma)}{\int P(\beta\gamma) \exp\left[-t_S(\beta\gamma)/\tau\right]\{1 - \exp\left[\Delta t(\beta\gamma)/\tau\right]\} d(\beta\gamma)}, \tag{2}$$

where $P(\beta\gamma)$ is the momentum distribution; $t_L(\beta\gamma)$, $t_S(\beta\gamma)$ are the flight times

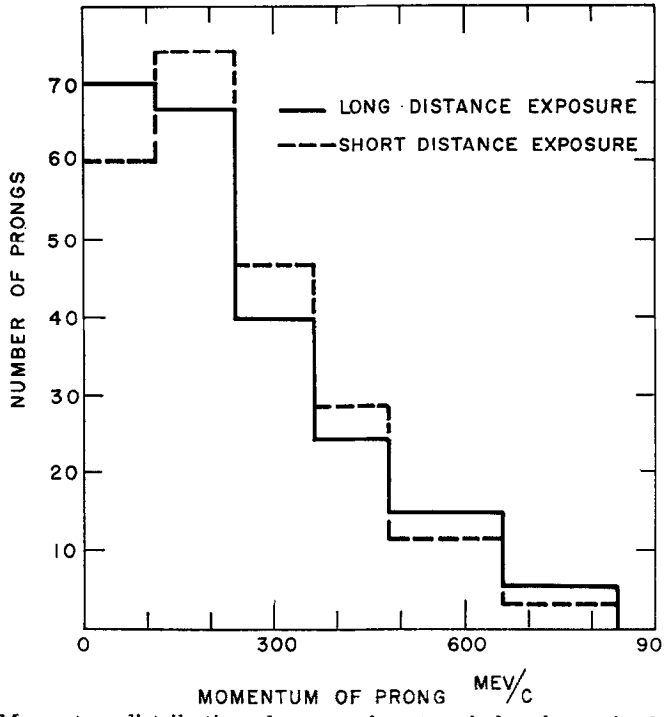

FIG. 11. Momentum distribution of prongs of neutron induced stars in the cloud chamber gas.

for the long and the short distance runs respectively for a K_2^0 of momentum $M\beta\gamma c$ and $\Delta t(\beta\gamma)$ is the time to traverse the cloud chamber. In Fig. 12 we have plotted the relation between R and τ as given by Eq. (2), using an intermediate and two extreme shapes for $P(\beta\gamma)$. These were computed by Sternheimer for associated production of YK pairs in a complex nucleus by incident 3.0-Bev protons. At large laboratory angles, the velocity spectra are quite insensitive to details of the transition matrix element. Applying Eq. (1) to Fig. 4 and using the $P(\beta\gamma)$ given by phase space and Fermi momentum distribution of the target nucleons leads to the result:[7]

$$\tau = 8.1^{+3.2}_{-2.4} \times 10^{-8} \text{ sec.} \tag{3}$$

The sensitivity of the result to the velocity distribution can be obtained from Fig. 12. Curves a and c represent the extreme spectra calculated by Sternheimer, curve b is the spectrum used above. The identified events permit an evaluation of the K^0 velocity in many cases. A distribution consisting of 30 such events

[7] This result is in agreement with a more preliminary value given by Bardon *et al.* (*14*).

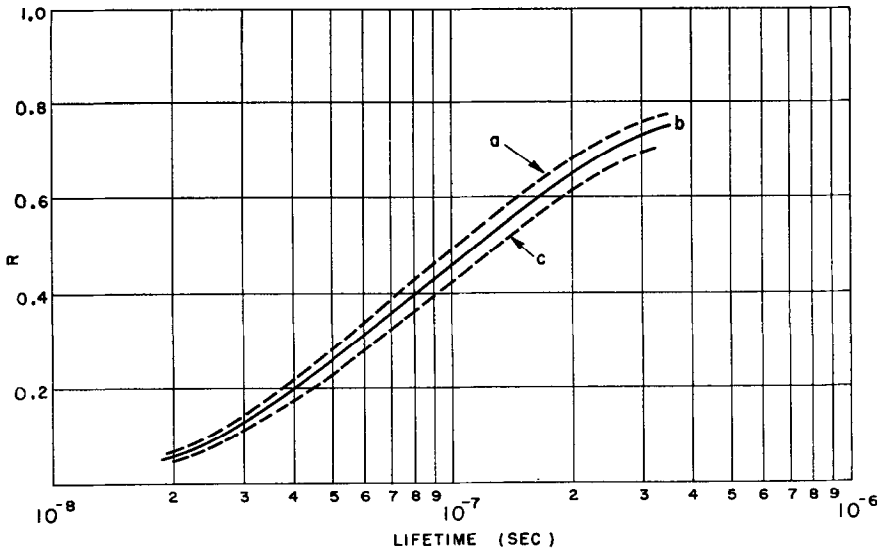

FIG. 12. Dependence of the K_2^0 lifetime on the ratio, R, of the yields in the two exposures. Curve a is computed with a K_2^0 energy spectrum derived from an energy-dependent matrix element of the form $\gamma^2 - 1$, Gaussian momentum distribution of the target nucleons and isotropic angular distribution in the center-of-mass system. Curve b is obtained from an energy-independent matrix element, Fermi momentum distribution and isotropic angular distribution. Curve c from energy-independent matrix element, Gaussian momentum distribution and cos θ angular dependence.

(also including those K_2^0's in which the double valued velocities differ by little) is in good agreement with Sternheimer's distributions. Clearly this distribution may contain serious bias.

B. Comparison with K^+ Decay

A phenomenological estimate of the K_2^0 lifetime can be obtained from the known data on K^+ lifetime (*31*) and branching ratios (*32*, *33*) by application of charge independence and the $\Delta T = \frac{1}{2}$ selection rule. (T = total isotopic spin). The K_2^0 decay rate is

$$R(K_2^0) = \frac{1}{\tau} = R(\pi^+\mu^-\nu) + R(\pi^+e^-\nu) + R(\pi^-\mu^+\nu) + R(\pi^-e^+\nu) + R(\pi^+\pi^-\pi^0) + R(\pi^0\pi^0\pi^0).$$

We assume that the partial ratio for the K_2^0 leptonic modes are the same as the corresponding K^+ rates. For the partial rates of the decays involving three pions, the isotopic spin formalism and charge independence, together with the

$\Delta T = \frac{1}{2}$ selection rule, is used to obtain a relation between the partial rates for decay of K^+ mesons and their counterparts in the decay of the neutral K mesons (*34*).

Then we obtain the lifetime:

$$\tau \simeq 5 \times 10^{-8} \text{ sec.}$$

Similar results have been obtained by Gell-Mann, and Okun using a specific model for the K meson decay interactions and by Marshak *et al.* (*35*).

SUMMARY AND REVIEW

The basic conclusions drawn from the Gell-Mann and Pais particle mixture theory are:

(1) Those K^0's produced in strong reactions, e.g., $\pi + N \rightarrow Y + K$, with positive strangeness, have equal probability of decaying via a "fast" K_1^0 mode or a slow K_2^0 mode. In a typical experiment (bubble chamber observation of $\pi - N$ collisions) where the observation time is $\sim 5 \times 10^{-10}$ sec, essentially all the K_1^0 decays take place within the chamber while none of the K_2^0 decays are observed. Thus one-half the hyperons produced in association with a K^0 will be accompanied by observable K_1^0 decays (including here $K_1^0 \rightarrow 2\pi^0$).

(2) The K_2^0 modes should be characterized by a unique lifetime, presumably $\gg 10^{-10}$ sec, and decay modes different from K_1^0. Thus, if a K^0 beam is observed at times long compared to the K_1^0 lifetime, only anomalous (not two pion) final states should be observed.

The confirmation of prediction (1) has been given by Eisler *et al.* (*27*). Further, two cases of associated production of a hyperon and K_2^0 have now been observed (*36*).

The present paper described the work done to test prediction (2). In this experiment the decay of the long-lived neutral K meson was detected in such circumstances as to give an unambiguous proof of the existence of this particle. Its decay modes were studied and the lifetime determined.

Following the Gell-Mann and Pais proposal, further consequences of the particle mixture theory were discussed by a number of authors (*37–42*). The important consequences of these considerations are briefly summarized:

(3) The strong interactions of the K_2^0 should be characteristic of both positive and negative strangeness (with equal probability). In particular particles in a K_2^0 beam should be capable of regenerating K_1^0 events by nuclear collisions (Pais-Piccioni effect) or interacting to produce hyperons.

(4) During the lifetime of the particles, there is an interference between the component K_0 and $\bar{K}_0$ states. This produces an oscillation in probability amplitude with frequency $\Delta m/\hbar$ where Δm is the $K_1^0 - K_2^0$ mass difference. Thus, the decay rate into any mode shared by K_1^0 and K_2^0 is not simply a sum of exponentials.

Evidence for (3) comes from emulsion exposures to neutral beams (*43*, *44*) from a propane bubble chamber exposure (*45*), from electronic study of K_2^0 interactions (*46*) and from the present experiment [see Lande, Lederman, and Chinowsky (*14*)]. No observations of (4) have yet been made.[8]

Experimental possibilities are still far from being exhausted. Study of the details of the three body leptonic modes offers new tools for the study of the weak interactions from determination of angular and momentum distributions and polarizations (*48*). No experiments have yet clearly demonstrated the interference effects or the K_1^0 regeneration. In fact, no one result can be said to have demonstrated the necessity of the K^0 particle mixture, although it is at present the only theory sufficient to explain all the observations.

The authors wish to acknowledge the collaboration of Prof. John Tinlot and Dr. Morton Fuchs in the collection and analysis of the photographs. Major contributions to scanning (see Fig. 2) were made by Mr. G. Impeduglia and Miss Julia Thatcher.

RECEIVED: August 1, 1958

REFERENCES

1. A. PAIS AND M. GELL-MANN, *Phys. Rev.* **97**, 1387 (1955).
2. C. S. WU, E. AMBLER, D. D. HOPPES, R. W. HAYWARD, AND R. P. HUDSON, *Phys. Rev.* **105**, 1413 (1957); R. L. GARWIN, L. M. LEDERMAN, AND M. WEINRICH, *Phys. Rev.* **105**, 1415 (1957); J. I. FRIEDMAN AND V. L. TELEGDI, *Phys. Rev.* **105**, 1681 (1957).
3. T. D. LEE, R. OEHME, AND C. N. YANG, *Phys. Rev.* **106**, 340 (1957).
4. L. W. ALVAREZ, H. BRADNER, P. FALK-VAIRANT, J. D. GOW, A. ROSENFELD, F. SOLMITZ, AND R. TRIPP, *Nuovo cimento* **5**, 1026 (1957).
5. M. N. WHITEHEAD, R. W. BIRGE, W. B. FOWLER, R. LANOU, AND W. M. POWELL, *Bull. Am. Phys. Soc.* Ser II, **1**, 24 (1958).
6. L. LANDAU, *Nuclear Phys.* **3**, 127 (1957).
7. R. GATTO, *Phys. Rev.* **106**, 168 (1957); S. TRIEMAN AND R. WYLD, *Phys. Rev.* **106**, 169 (1957).
8. F. EISLER, R. PLANO, N. SAMIOS, M. SCHWARTZ, AND J. STEINBERGER, *Nuovo cimento* **10**, 1700 (1957).
9. S. WEINBERG, *Phys. Rev.* **110**, 782 (1957).
10. R. THOMPSON, *Progress in Cosmic Ray Physics* **3**, 255 (1956).
11. M. GOOD, in "Proceedings of the Eighth Annual High Energy Conference, Geneva, 1958." To be published.
12. H. BLUMENFELD, E. T. BOOTH, L. M. LEDERMAN, AND W. CHINOWSKY, *Phys. Rev.* **102**, 1184 (1956).
13. J. BALLAM, M. GRISARU, AND S. B. TRIEMAN, *Phys. Rev.* **101**, 1438 (1956); G. G. SLAUGHTER, E. M. HARTH, AND M. M. BLOCK, *Phys. Rev.* **109**, 2111 (1958); C. D. D'ANDAU, R. ARMENTEROS, A. ASTIER, H. C. DESTAEBLER, B. P. GREGORY, L. LEPRINCE-RINGUET, F. MULLER, C. PEYROU, AND J. TINLOT, *Nuovo cimento* **6**, 1135 (1957); J. A. KADYK, G. H. TRILLING, R. LEIGHTON, AND C. D. ANDERSON, *Phys. Rev.* **105**, 1862 (1957).

[8] Some interesting proposals have been made (see Ref. *47*).

14. K. LANDE, E. T. BOOTH, J. IMPEDUGLIA, L. M. LEDERMAN, AND W. CHINOWSKY, *Phys. Rev.* **103,** 1901 (1956); K. LANDE, L. M. LEDERMAN, AND W. CHINOWSKY, *Phys. Rev.* **105,** 1925 (1957); M. BARDON, M. FUCHS, K. LANDE, L. M. LEDERMAN, W. CHINOWSKY, AND J. TINLOT, *Phys. Rev.* **110,** 780 (1958).
15. G. FRIEDLANDER AND J. M. MILLER (private communication of unpublished results).
16. H. BLUMENFELD, W. CHINOWSKY, AND L. M. LEDERMAN, *Nuovo cimento* **8,** 296 (1958).
17. R. THOMPSON, *Nuovo cimento* **10,** 735 (1955).
18. C. P. SARGENT, M. RINEHART, K. ROGERS, AND L. M. LEDERMAN, *Phys. Rev.* **99,** 885 (1955).
19. D. O. CALDWELL AND YASH PAL, *Rev. Sci. Instr.* **27,** 633 (1956).
20. W. O. LOCK, in "CERN Symposium Report," Vol. 2, p. 384. CERN, Geneva, 1956.
21. L. RIDDIFORD, in "Proceedings of the Seventh Annual Rochester Conference on High Energy Physics," p. II-59. Interscience, New York, 1957.
22. W. A. WALLENMEYER, *Phys. Rev.* **105,** 1058 (1957).
23. E. FOWLER, W. FOWLER, R. SHUTT, W. THORNDIKE, AND W. WITTEMORE, *Phys. Rev.* **91,** 135 (1953).
24. C. PEYROU, in "Proceedings of the Sixth Annual Rochester Conference on High Energy Physics." Interscience, New York, 1956.
25. A. BORSELLINO, *Phys. Rev.* **89,** 1023 (1953).
26. P. T. MCCORMICK, D. G. KEIFFER, AND G. PARZEN, *Phys. Rev.* **103,** 29 (1956).
27. F. EISLER, R. PLANO, N. SAMIOS, M. SCHWARTZ, AND J. STEINBERGER, *Nuovo cimento* **5,** 1700 (1957).
28. R. DALITZ, *Phys. Rev.* **99,** 915 (1955).
29. J. A. KADYK, G. H. TRILLING, R. B. LEIGHTON, AND C. D. ANDERSON, *Phys. Rev.* **105,** 1862 (1957).
30. B. P. GREGORY, in "Proceedings of the International Conference on Elementary Particles, Padua-Venice, 1957." *Suppl. Nuovo cimento* (to be published).
31. V. FITCH AND R. MOTLEY, *Phys. Rev.* **101,** 496 (1956).
32. R. W. BIRGE, D. H. PERKINS, J. R. PETERSON, D. H. STORK, AND M. N. WHITEHEAD, *Nuovo cimento* **4,** 834 (1956).
33. C. O'CEALLIGH, in "Proceedings of the Seventh Annual Rochester Conference on High Energy Nuclear Physics." Interscience, New York, 1957.
34. R. DALITZ, in *Proc. Phys.* Soc. **A69,** 527 (1956).
35. M. GELL-MANN (private communication, 1956); L. B. OKUN, post-deadline paper to the American Physical Society Meeting at Stanford, December, 1957; to be published; R. MARSHAK, in "Proceedings of the Eighth Annual High Energy Conference, Geneva, 1958." To be published.
36. F. EISLER, R. PLANO, N. SAMIOS, J. STEINBERGER, AND M. SCHWARTZ, *Phys. Rev.* **110,** 226 (1958), and private communication.
37. A. PAIS AND O. PICCIONI, *Phys. Rev.* **100,** 1487 (1955).
38. K. M. CASE, *Phys. Rev.* **103,** 1449 (1956).
39. M. L. GOOD, *Phys. Rev.* **106,** 591 (1957).
40. S. TRIEMAN AND R. G. SACHS, *Phys. Rev.* **103,** 1545 (1956).
41. W. F. FRY AND R. G. SACHS, *Phys. Rev.* **109,** 2212 (1958).
42. M. L. GOOD, *Phys. Rev.* **110,** 550 (1958).
43. M. BALDO-CEOLIN, C. C. DILWORTH, W. F. FRY, W. D. B. GREENING, H. HUZITA, S. LIMENTANI, AND A. E. SICHIROLLO, *Nuovo cimento* **6,** 130 (1957).
44. R. AMMAR, J. I. FRIEDMAN, R. LEVI-SETTI, AND V. TELEGDI, *Nuovo cimento* **5,** 1801 (1957).

45. W. B. Fowler, R. Lander, and W. M. Powell, *Bull. Am. Phys. Soc.* Ser. II, **2,** 236 (1957).
46. W. K. H. Panofsky, V. Fitch, R. Motley, and W. Chesnut, *Phys. Rev.* **109,** 1353 (1958).
47. V. Fitch (private communication); W. Fry and R. G. Sachs, *Phys. Rev.* **109,** in press (1958).
48. A. Pais and S. Trieman, *Phys. Rev.* **105,** 1616 (1956); S. Furuichi, *Nuovo cimento* **7,** 269 (1958); J. J. Sakurai, *Phys. Rev.* **109,** 980 (1950) for references to earlier work.